



Collision Integrals for Nitrogen and Hydrogen Ionized Gas: The Exact Values and Assessment of Approximations

Marcin Buchowiecki¹ · Péter Szabó^{2,3}

Received: 23 August 2022 / Accepted: 9 November 2022 / Published online: 8 December 2022
© The Author(s) 2022

Abstract

Collision integrals are calculated for the $H-N^+$, $N-H^+$, $N^{2+}-H$, and N^+-H^+ interactions in the temperature range of 1000–60,000 K. The resulting collision integrals were fitted to simple functional forms. The applicability of commonly used approximations for calculation of the collision integrals is verified. Those approximations are simplification of exact potentials (especially the repulsive ones), use of polarizability potential for atom–ion interaction, and use of Coulomb screened potential for ion–ion interaction. The reported collision integrals are based on the ab initio calculated points of the potential energy curves, so that the error of fitting the points with analytical potential energy function is not present.

Keywords Potential energy curves · Collision integrals · Ionized gas · Plasma · Debye screening · Atom–atom interactions · Atom–ion interactions · Ion–ion interactions

Introduction

The collision integrals of interacting atoms and ions are the basis of modelling of the transport properties of high temperature gases and plasmas in the Chapmann-Enskog theory [1]. The role of atomic diffusion is recently gaining recognition in stellar astrophysics [2]. The problem in calculations of the collision integrals is quality of the underlying potential energy curves (PECs), they are often fitted to analytical functional forms which are designed for description of attractive potentials and are not appropriate to describe, the equally important for the scattering process, curves of mainly repulsive character [3].

This research has two aspects, computational and theoretical. The computational one is the crucial one because the collision integrals are sensitive to PECs. The present study applies the best computational practice that is—the high precision quantum chemistry methods for potential energy at various interatomic distances and calculation of collision

✉ Marcin Buchowiecki
marcin.buchowiecki@usz.edu.pl

¹ Institute of Physics, University of Szczecin, Wielkopolska 15, 70-451 Szczecin, Poland

² Department of Chemistry, KU Leuven, Celestijnenlaan, 200F, 3001 Leuven, Belgium

³ Royal Belgian Institute for Space Aeronomy (BIRA-IASB), Avenue Circulaire 3, 1180 Brussels, Belgium

integrals on the basis of those points (without fitting to functional form of PECs) with the developed Python code using numerical methods implemented in the SciPy package [4].

The theoretical aspect is the assessment of the commonly used approximations that is: (1) the difference of collision integrals based on the ab initio points with the values based on the analytical PECs currently in use, (2) the quality of exponential versus exact description of the repulsive PECs, (3) the quality of description of interaction of neutral atom with ionized atom by polarizability (polarization) potential (with respect to the known shapes of PECs this approximation is not correct even qualitatively), and finally (4) the use of Coulomb screened potential for ions interaction.

The present research is the continuation of study of the collision integrals for the neutral nitrogen and hydrogen atoms [3]. The other studies of various systems containing nitrogen and hydrogen atoms [3, 5–7] use approximations mentioned above, which is usually necessary because of the lack of the high excited electronic states. The available spectroscopic constants are not sufficient for the high quality overall description of PEC, in particular repulsive ones which may be not available at all. In the present study, the high quality PECs are calculated eliminating this problem.

The studies of collision integrals by Stallcop et al. of N–H interaction [8], N–N, O–O, and N–O interactions [9], and $N^+–N^+$, $N^+–O^+$, and $O^+–O^+$ interactions [10] are few (perhaps even the only ones) based directly on the ab initio quantum chemistry methods whereas, for the high quality of collision integrals, such approach should become standard. The authors of the study of N–N, O–O, and N–O collisions [9] mention that uncertainty is introduced by fitting to ab initio points of PECs and that the second order corrections to transport properties introduce error of less than 1%.

Usually only the states of lower electronic excitation are well represented by the various analytical forms of PECs, but excited (in particular repulsive) states are equally important for collision integrals so that using interpolation and extrapolation of ab initio points instead of analytical PECs is a significant ingredient of highly accurate calculations.

In this study, calculations of NH^+ and NH^{2+} collision integrals were based on ab initio calculated PECs since the attractive ones currently in use [5, 7, 11] are based on old data [12] or are based on simplified models such as polarizability model [11], and the repulsive ones are described by a simple exponential function already known to introduce significant inaccuracy for the N–H interaction [3].

The studies done so far also did not take into account excited states of atoms, which are also dealt with in the present study. Rare examples when excited states of atoms were taken into account are studies of collision integrals of oxygen atoms interactions [13, 14], nitrogen atom interactions [13, 15] and N–H interactions [3].

The importance of excited atoms depends on their number which increases with temperature and in plasmas at any temperature excited atoms are created by interaction with electrons but details depends on actual state of plasma.

In case of interaction of two ions (lower energy states of the NH^{2+} system) the Coulomb screened potential is the commonly used standard [5, 7, 16, 17], which is correct only at higher interatomic distances (ions can be treated as a point charges). Probably the only case of study in which actual interaction of ions (calculated by quantum chemistry methods) was taken into account is the publication of Stallcop et al. [10], which compares collision integrals for nitrogen and oxygen ions based on the Coulomb and real screened potentials. The application of real potentials was found to be especially important at high temperatures. In the present study also such comparison will be done (for nitrogen and hydrogen ions interaction for the ground and excited states of ions) and justification of such procedure will be given.

Often the ab initio quantum chemical studies of potential of species in question were done for spectroscopy [18], but some also report energy points of calculates states [19]. Dications have particular shape of the ground state PEC [20] and there are some studies of the ground and excited states [21, 22], also analytical PEC was developed [23].

The non-adiabatic effects on PECs in scattering events can also influence the resulting collision integrals. Some non-adiabatic processes result in non-elastic scattering which will describe events other than transport. Other non-adiabatic processes may influence transport properties which are based on elastic scattering; there are almost no such studies with the exception of spin-orbit coupling which turns out to be small in the known cases [24, 25].

The section two of this article presents the methodology for the ab initio calculations of PECs and collision integrals calculations (theoretical and computational aspects), in section three the results are presented and discussed, and in section four the final conclusions of the study are presented.

This study use atomic units, except for collision integrals which are traditionally given in \AA^2 .

Methodology

Ab Initio Calculations of Potential Energy Curves

The MOLPRO-2020 package [26] was employed for the quantum chemical calculations. All of the potential energy curves are obtained with the internally contracted explicit correlated multireference configuration interaction method (icMRCI-f12) with Davidson correction using the aug-cc-pVQZ-f12 basis set. We used the C_{2v} symmetry group for all the calculations. The reference wavefunction for the icMRCI-f12 calculations is constructed by using the complete active space self-consistent field (CASSCF) method with an active space consisting of 7 electrons on 9 orbitals ($4a_1, 2b_1, 2b_2, 1a_2$) for NH^+ molecule, and 6 electrons on 9 orbitals ($4a_1, 2b_1, 2b_2, 1a_2$) for NH^{2+} molecule, respectively.

Calculations of Collision Integrals

Deflection angle of scattered particles (atoms or ions) interacting with the potential energy function $V(r)$ is calculated in the classical theory as [27]

$$\chi(b, \gamma, T) = \pi - 2b \int_{r_c}^{\infty} \frac{dr}{r^2 \sqrt{1 - \frac{b^2}{r^2} - \frac{V(r)}{kT\gamma^2}}}, \tag{1}$$

where b is the impact parameter, r_c is the classical turning point (distance of closest approach), and $\gamma^2 = \mu g^2 / (2kT)$ (μ —reduced mass, g —relative velocity, k —Boltzmann constant, T —temperature).

Reduced collision integrals are then expressed as [1]

$$\sigma^2 \Omega^{(l,s)*} = \frac{4}{(s+1)! \left[1 - \frac{1+(-1)^s}{2} \frac{1+l}{1+l} \right]} \int_0^{\infty} \int_0^{\infty} e^{-\gamma^2} \gamma^{2s+3} (1 - \cos^l \chi(b, \gamma, T)) b \, db \, d\gamma. \tag{2}$$

If two particles interact according to more than one PEC, the collision integral is defined as the weighted average (statistical weights according to molecular term symbols).

Tests of the Code on the Lennard-Jones Potential

In the computational approach with SciPy library of Python programming language, the PEC $V(r)$ is not given analytically but interpolated with `interp1d` command for cubic spline interpolation (with option of extrapolation) to fit calculated energy points.

For one dimensional integration for deflection angle (Eq. 1) the `quad` command calls Fortran library QUADPACK of adaptive quadratures (relative error tolerance is set to 0.01). The classical turning point (lower integration limit) is calculated with the `optimize.root_scalar` command with the method `brenth`.

The `nquad` command (relative error tolerance is set to 0.01) is used for the double integral over b and γ .

The Lennard-Jones potential

$$V_{LJ}(r) = 4D_e \left[\left(\frac{\sigma}{r} \right)^{12} - \left(\frac{\sigma}{r} \right)^6 \right], \quad (3)$$

with $D_e = 0.1$, and $\sigma = 1.5$, for which the high quality collision integrals are known, is used for testing the code.

Table 1 shows that the chosen methods and settings in case of the analytical form of the Lennard-Jones PEC results with four (at lower temperatures) or five (at higher temperatures) significant digits agreement with high precision values of Kim and Monroe [28]. The values based on cubic spline interpolation of 73 points of exact PEC are usually in four significant digits agreement with the reference Kim and Monroe values.

The extrapolation resulted in the incorrect long range tail of PEC (this is important for the accuracy of deflection angle) and setting the potential exactly zero at interatomic distances longer than 30 bohr results in high quality results mentioned above.

According to the obtained accuracy, the present study will show four significant digits for the collision integrals. In the light of discrepancies seen for the N–N or N–H collision integrals [3, 29] the accuracy of three significant digits is satisfactory.

Finally, be aware that when PEC as integration of ab initio is used instead of analytic function, computational times are increased many times.

Table 1 The Lennard-Jones $\Omega^{(1,1)*}$ and $\Omega^{(2,2)*}$ collision integrals based on analytic PEC of Eq. 3 (PEC) and interpolation of exact energy points (fit) compared with Kim and Monroe values (KM)

T^*	T/K	$\Omega^{(1,1)*}$ PEC/fit	$\Omega^{(1,1)*}$ KM	$\Omega^{(2,2)*}$ PEC/fit	$\Omega^{(2,2)*}$ KM
0.1	3158	4.0118/4.0096	–	4.1015/4.1010	–
0.3	9473	2.6501/2.6496	2.6500	2.8440/2.8418	2.8437
0.6	18,947	1.8772/1.8768	1.8769	2.0842/2.0837	2.0848
1.0	31,578	1.4398/1.4395	1.4398	1.5932/1.5927	1.5932
2.0	63,155	1.0754/1.0753	1.0754	1.1758/1.1756	1.1758
10	315,775	0.74224/0.74203	0.74224	0.82437/0.82413	0.82437

The reduced temperatures (T^*) and actual temperatures in Kelvins (T/K) are given

Discussion of Collision Integrals

The PECs obtained from ab initio calculations are shown for singly ionized systems (N–H⁺ and H–N⁺ interactions) in Fig. 1 and for doubly ionized systems (H–N²⁺ and H⁺–N⁺ interactions) in Fig. 2. In the following tables the collision integrals based on those PECs are reported and compared with the ones based on the PECs reported in Ref. [5]. The polarizability approximation and screened ion–ion interaction are discussed in the separate subsections.

The importance of high quality PECs for collision integrals was already discussed for both attractive and repulsive (which are typically approximated with simple exponential function) PECs [3, 29].

Tables 2 and 4 present $\sigma^2\Omega^{(1,1)*}$ collision integrals for attractive interactions based on the MRCI curves with the ones based on the curves used in ref. [5]. It can be seen that correction provided by the newly calculated high quality PECs is 2–10% ($X^2\Pi$), 4–16% ($a^2\Sigma^-$), and 9–28% ($4\Sigma^-$). This can be compared with 0.7–27% correction for attractive curve of the N–H system [3]. The highest discrepancy can be at low, intermediate or high temperature in the range considered (1000–60,000 K).

For the $a^4\Sigma^-$ state some numerical problems caused suspicious increase of the values of collision integrals at lowest temperatures (much higher than reported for other attractive PECs; see Table 4). They were recalculated with the following PEC:

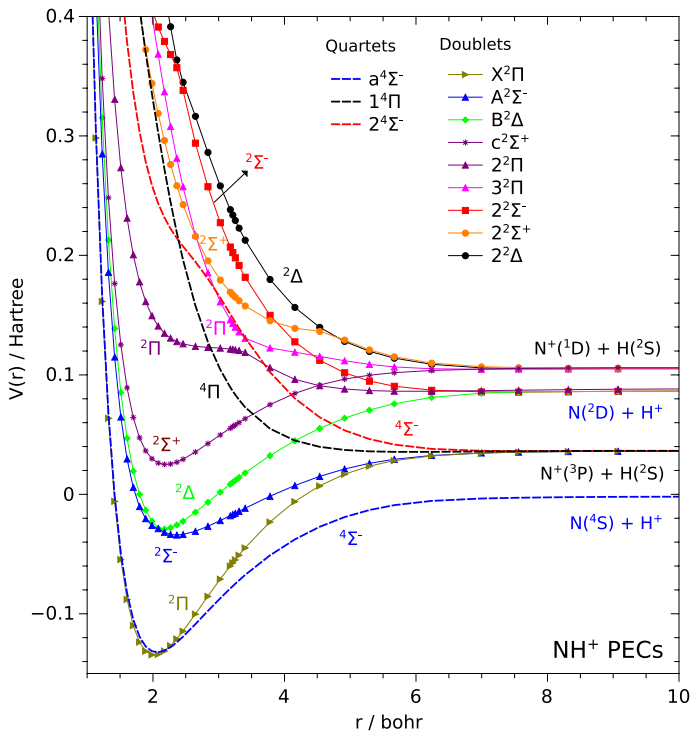


Fig. 1 Potential energy curves of the NH⁺ molecule calculated with icMRCI-f12 method and aug-cc-pVQZ-f12 basis set

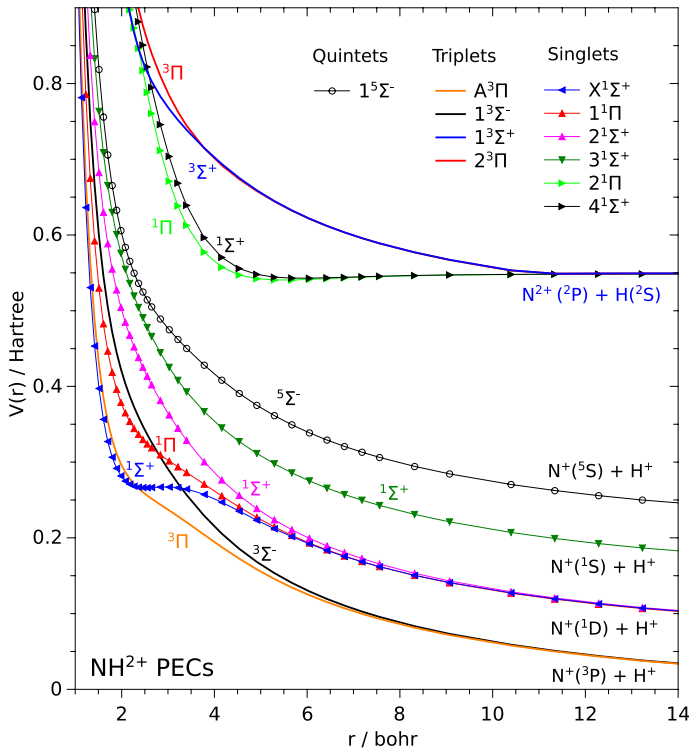


Fig. 2 Potential energy curves of the NH_2^+ molecule calculated with icMRCI-f12 method and aug-cc-pVQZ-f12 basis set

Table 2 Collision integrals $\sigma^2 \Omega^{(1,1)*}$ for the attractive PECs of the H–N⁺ interaction dissociating to the ground state atoms/ions (MRCI) compared with the results based on PECs given in Ref. [5]

T/K	$X^2\Pi$ MRCI	$X^2\Pi$ [5]	$a^2\Sigma^-$ MRCI	$a^2\Sigma^-$ [5]
1000	16.10	17.40	16.51	15.59
2000	13.56	14.20	13.50	12.41
5000	10.54	10.27	8.067	7.038
10,000	7.209	6.828	4.109	3.542
20,000	3.772	3.560	1.858	1.645
30,000	2.373	2.230	1.185	1.080
40,000	1.681	1.568	0.8839	0.8240
60,000	1.037	0.9466	0.6111	0.5869

Compare Fig. 1 for the term symbols

$$V(r) = \frac{\exp(-3.80048r)(1 + 0.303439/r) + \exp(-0.96574r)(1/r - 0.513688r)}{1.03355 - 0.783200 \exp(-r)(1 + r + r^2/3)}, \quad (4)$$

which describes the ab initio MRCI calculated energies well. This comparison confirms that higher temperatures are in agreement and in final results the 1000 K and 2000 K values will be replaced with this new values, which can be assumed correct because the

difference with the values based on the other PEC are not in excessive disagreement (now disagreement is comparable to the values reported for other attractive PECs). Note also that calculations on the analytical form of PEC are many times faster and can serve as a comparison of the piecewise interpolated curve if no other results are available. It also reminds of the difficulties of the collision integrals, especially at low temperatures where substantial orbiting can occur (quantum mechanical or semi-classical approach is more adequate for those temperatures); on the other side the lowest temperatures reported are not very important in the situation where non-negligible portion of molecules are dissociated into atoms/ions which collisions are described in this study.

For the repulsive PECs, Table 3 gives $\sigma^2\Omega^{(1,1)*}$ collision integrals, and the corrections are 1–39% (${}^4\Pi$) and 2–32% (${}^4\Sigma^-$). The exponential approximation is of bad quality, so that is it understandable that high corrections are at both low temperatures (39% and 27.5% at 1000 K for ${}^4\Pi$ and ${}^4\Sigma^-$ respectively) and high temperatures (20% and 32% at 60,000 K for ${}^4\Pi$ and ${}^4\Sigma^-$ respectively); note also that around 20,000 K correction is small because at low temperature correction is positive and at high temperature is negative. In case of N–H interaction corrections for the repulsive curves are between 7 and 27% [3].

The MRCI PECs of the discussed states (solid lines) are compared with the ones of Ref. [5] (dashed lined) in Fig. 3 for H–N⁺ interaction and in Fig. 4 for the N–H⁺ interaction.

Ion–Atom Interactions (H–N⁺, N–H⁺, and H–N²⁺) and Polarizability Approximation

For the ion–atom interactions, simplification of the interaction with polarizability (polarization) model is often used. Sometimes this approximation is used for singly charged ions [11, 30] but typically this model is used for ions with higher charge [5].

The polarizability potential

$$V(r) = -\frac{Ze^2\alpha_X}{8\pi\epsilon_0r^4}, \tag{5}$$

with polarizability of atom X, α_X and ion charge Z. The formulas for collision integrals for this potential are known [31, 32], the formula for $\sigma^2\Omega^{(1,1)*}$ integral is

$$\sigma^2\Omega^{(1,1)*} = 424.443Z\sqrt{\alpha_X/T}, \tag{6}$$

Table 3 Collision integrals $\sigma^2\Omega^{(1,1)*}$ for the repulsive PECs of the H–N⁺ interaction dissociating to the ground state atoms/ions (MRCI) compared with the results based on PECs given in Ref. [5]

T/K	${}^4\Pi$ MRCI	${}^4\Pi$ [5]	${}^4\Sigma^-$ MRCI	${}^4\Sigma^-$ [5]
1000	7.028	5.055	9.866	7.737
2000	5.144	4.265	7.908	6.392
5000	3.693	3.325	5.856	4.815
10,000	2.849	2.693	4.392	3.773
20,000	2.105	2.129	2.922	2.861
30,000	1.705	1.831	2.136	2.388
40,000	1.438	1.633	1.663	2.080
60,000	1.096	1.374	1.1414	1.683

Compare Fig. 1 for the term symbols

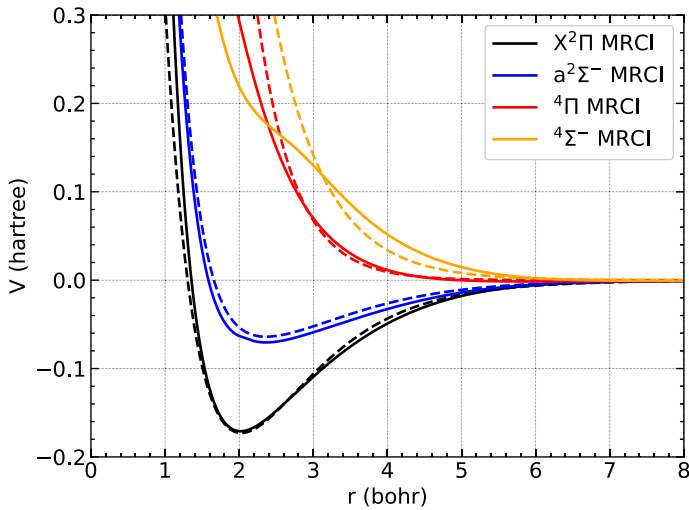


Fig. 3 The MRCI PECs for the H-N^+ interactions dissociating to the ground state atoms/ions. Dotted lines shows curves given in Ref. [5]

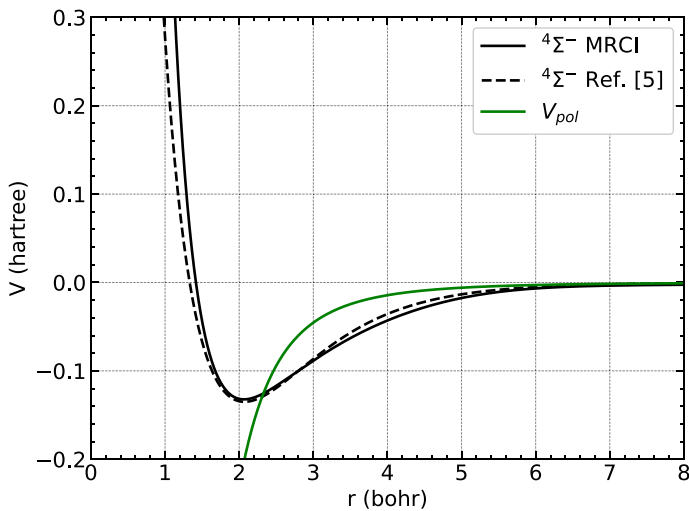


Fig. 4 The MRCI PECs for the N-H^+ interaction dissociating to the ground state nitrogen atom. Dotted line shows curve given in Ref. [5]. Polarizability potential (V_{pol}) is given for comparison

with polarizability of nitrogen atom $\alpha_N = 1.0904 \text{ \AA}^3$ and hydrogen atom $\alpha_H = 0.66668 \text{ \AA}^3$ [5].

Note that polarizability potential is not even qualitatively (repulsive part of potential is not present) correct description the actual potential neither in case of singly charged ion (Fig. 4 for N-H^+ interaction) and doubly charged ion (Fig. 5 for H-N^{2+}). The polarizability potential describes only attraction of ion with polarized atom but, at

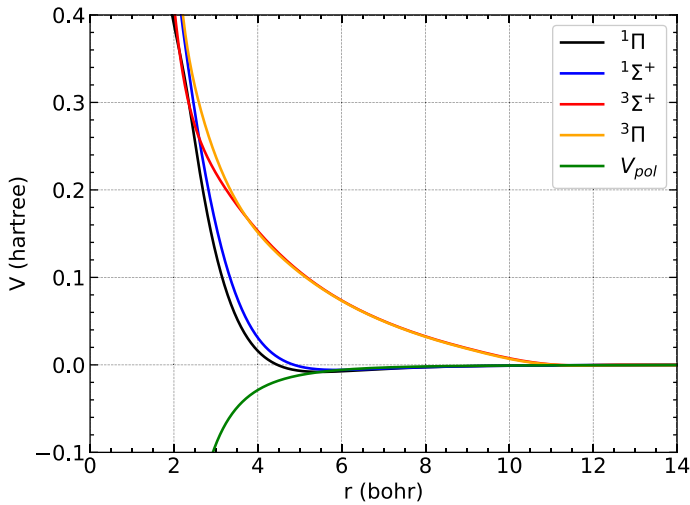


Fig. 5 The MRCI PECs for the H–N²⁺ interactions dissociating to the ground states atoms/ions. Polarizability potential (V_{pol}) is given for comparison

Table 4 Collision integrals $\sigma^2 Q^{(1,1)*}$ for the N–H⁺ interaction on the attractive $a^4 \Sigma^-$ PEC (MRCI) compared with the results based on PECs given in Ref. [5]

T/K	$a^4 \Sigma^-$ MRCI	[5]	polarizability
1000	33.12/20.91	16.58	14.02
2000	19.32/17.06	13.35	9.911
5000	11.24/11.52	9.259	6.268
10,000	6.442/6.570	5.695	4.432
20,000	3.031/3.047	2.779	3.133
30,000	1.866/1.866	1.709	2.559
40,000	1.325/1.322	1.198	2.216
60,000	0.8377/0.8355	0.7291	1.809

Compare Fig. 1 for the term symbol. Values of polarizability approximation are also given

inter-atomic distance small enough, the interaction always becomes repulsive. Additionally, interaction ion-atom is often described by more than one PEC (Fig. 5).

How polarizability approximation works in practice can be seen: in Table 4 for N–H⁺ (inaccuracy exceeding multiplier two at some temperatures), in Table 5 for H–N⁺ (moderate inaccuracy at most temperatures), and in Table 6 for H–N²⁺ (note in particular very high discrepancies at 2000 K and 5000 K). According to what is seen on the plots of PECs very significant inaccuracies are not surprising.

Ion-ion Interaction (H⁺–N⁺) and Coulomb Screening

In ionized gas, screening of ions by other charged particles (electrons and ions) have to be taken into account. It can be learned from derivation of Debye-Huckel theory that the exponential screening factor (dependent on the Debye length λ_D) appears together with

Table 5 Collision integrals $\sigma^2 \Omega^{(1,1)*}$ for the H–N⁺ interaction dissociating to the ground state atoms/ions (MRCI)

T/K	MRCI	polarizability
1000	10.73	10.96
2000	8.557	7.750
5000	6.181	4.902
10,000	4.301	3.466
20,000	2.630	2.451
30,000	1.891	2.001
40,000	1.480	1.733
60,000	1.039	1.415

Values of polarizability approximation are also given. See Fig. 1 for the PECs used

Table 6 Collision integrals $\sigma^2 \Omega^{(1,1)*}$ for the H–N²⁺ interaction dissociating to the ground state atoms/ions (MRCI)

T/K	MRCI	polarizability
1000	27.02	21.92
2000	22.14	15.50
5000	15.93	9.803
10,000	11.09	6.932
20,000	6.750	4.902
30,000	4.748	4.002
40,000	3.617	3.466
60,000	2.409	2.830

Values of polarizability approximation are also given. See Fig. 2 for the PECs used

the $1/r$ functional form of the potential, it is called the screened (or shielded) Coulomb potential $e^{-r/\lambda_D}/r$ [33]. Without the screening, the long range tail of Coulomb type leads to divergence. Because of ionization, the ions at long distances are screened and this screening has to be applied [34].

Actual potential for H⁺–N⁺ collisions is not of the Coulomb type but can have much more complicated structure (minimum and maximum may be present as in the ground state of NH²⁺; see Fig. 2). Note that the ground state PEC of NH²⁺ molecule do not correspond to the ground state nitrogen ion N^{+(3P)} (hydrogen cation is a proton with no electronic states); it means that for atomic ionized gas in equilibrium, the most important are the interactions related to the ground state nitrogen ion, moreover ions can interact by more than one PEC which should be taken into account in the exact description.

For interaction of ions, complete set of PECs is needed but the studies of doubly ionized systems, especially with excited electronic states, are rare [35]. Note also that analytical PECs, if given, are focused on the chemically relevant region of energy well and are not correct for higher inter-atomic distances [23].

The exponential screening can be included by the *ad hoc* correction

$$V(r) = V_{\text{H}^+ - \text{N}^+}(r)e^{-r/\lambda_D}, \quad (7)$$

which was proposed in Ref. [10] and should be satisfactory for the large Debye lengths; also other applications of such procedure for non-Coulomb potentials are known [36, 37].

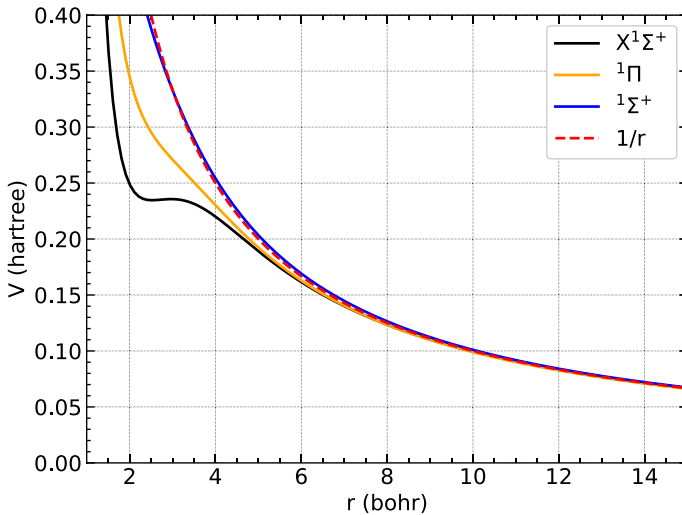


Fig. 6 The PECs dissociating to the $N^{+(1D)}$ nitrogen ion (first excited state) compared with the Coulomb potential ($1/r$). Each curve possess long range tail described exactly by the Coulomb potential

Figure 6 shows differences of the Coulomb and the calculated MRCI interaction potentials of the $N^{+(1D)}$ and H^+ ions; two of these curves diverge from the Coulomb one but one is almost exactly of Coulomb type. All the curves at larger inter-atomic distance follow exactly $1/r$ Coulomb curve because at long distances the electron clouds do not interact and ions can be treated as the point charges.

For two PECs shown in Fig. 6 which are not of Coulomb type, it was verified that for a very broad interval of Debye length values, the Poisson equation of Debye-Huckel theory [32] is satisfied with good accuracy by the MRCI screened potentials if $r > 2.5$, so that in that region the Coulomb screened potential (which fulfills that equation exactly) can be replaced with the exact MRCI one. The formal correctness mentioned above is presented in Fig. 7 (for Debye length 50 bohr) which presents fulfillment of the Poisson equation of the Debye-Huckel theory as the value of $P(r) = (V(r) \exp(-r/\lambda_D)r)''/r - V(r) \exp(-r/\lambda_D)/\lambda_D^2$ which should be close to zero.

For small inter-atomic distances ($r < 2.5$ bohr in this study, according to discussed Poisson equation) the screening should not be applied [33]; the unscreened MRCI potential is then correct in that region. Such theoretically preferred piecewise potential (exact unscreened below 2.5 bohr and exact screened above), with interpolated discontinuity, is shown for $\lambda_D = 10$ in Fig. 8 and for $\lambda_D = 50$ in Fig. 9 where discontinuity is negligible. The larger is the Debye length, the discontinuity is smaller and overall agreement with MRCI screened (for all inter-atomic distances) potential better. The conclusion is that exact screened potential (i.e. *ad hoc* correction) is a good approximation to justified above option (i.e. piecewise one) and the larger is the Debye length the better exact screened PEC gets and it is always better than the Coulomb screened potential.

What was called the small inter-atomic distance ($r < 2.5$) is still twice larger than radius of atomic nitrogen, so that the PEC is not modified by plasma effects below that value—the influence on electronic structure of the system do not have to be considered; it have to be considered in dense plasmas [38–40].

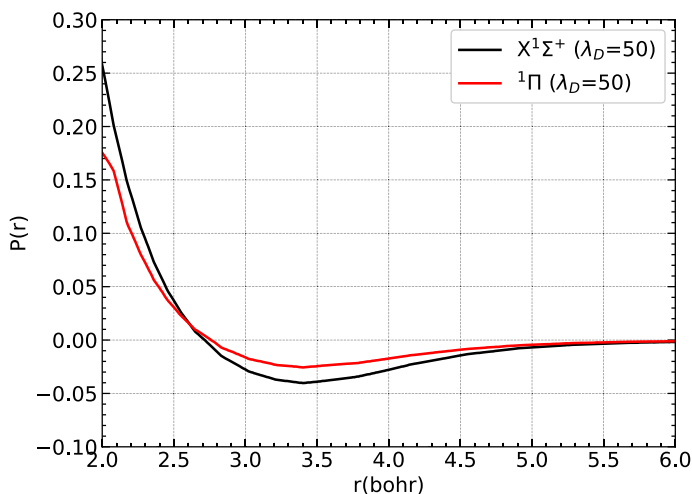


Fig. 7 Fulfillment of the Poisson equation of Debye-Huckel theory ($P(r) = 0$ condition) for $X^1\Sigma^+$ and $^1\Pi$ states (shown in Fig. 6). Intermediate value of Debye length $\lambda_D = 50$ was used

Table 7 compares Coulomb and the MRCI PECs based $\sigma^2\Omega^{(1,1)*}$ collision integrals calculated with the Python code with the use of lengths reduced with the Debye length ($r^* = r/\lambda_D$, $b^* = b/\lambda_D$). The Coulomb interaction is slowly decaying so that the interpolation with $1/r$ function based on last five calculated points had to be used to obtain dissociation energies. That reduction removes the possible numerical problems related to slowly decaying long range potential tail at large Debye lengths. The code also allows to calculate any collision integral by simply setting temperature and Debye length; the file is given as supplementary material.

The Coulomb description of ions interaction is not correct at higher energies (and increase with energy), it is seen in Table 7 that at higher temperatures collision integrals based on the exact interactions diverge from the Coulomb ones. Also for smaller Debye lengths, the use of the exact PEC is more important (the quality of Coulomb interaction decreases).

Conclusions

Collision integrals were calculated, and reported as a fits to simple analytical functions at temperatures 1000–60,000 K, on the basis of newly calculated high quality ab initio potential energy curves describing dissociation of both ground and excited states of atoms and ions. The quality of commonly used approximations were assessed with the following conclusions:

1. the quality of both attractive and repulsive PECs is crucial,
2. polarizability approximation for atom–ion description is not correct even qualitatively, and the results show that it should be discouraged at all situations; however, the problem is diminished by the fact that it is typically used for the less important cases of multiply charged ion interactions with atoms,

Table 7 Collision integrals $\sigma^2\Omega^{(1,1)*}$ of exponentially screened potentials: the Coulomb PEC ($1/r$), the ground state molecule ($X^1\Sigma^+$), the $^1\Pi$ state dissociating to the same states of ions as the ground state molecule ($^1\Pi$), followed by the values for four interactions given in Fig. 2 dissociating to the four lowest states of nitrogen ion respectively ($N^+(^3P)-H^+$, $N^+(^1D)-H^+$, $N^+(^1S)-H^+$, $N^+(^5S)-H^+$)

T/K	1/r	$X^1\Sigma^+$	$^1\Pi$	$N^+(^3P)-H^+$	$N^+(^1D)-H^+$	$N^+(^1S)-H^+$	$N^+(^5S)-H^+$
$\lambda_D = 10$							
1000	136.1	136.1	136.1	136.1	136.1	136.1	136.1
5000	43.65	43.57	43.41	43.60	43.58	43.63	43.64
10,000	23.56	23.29	23.28	23.47	23.40	23.51	23.51
30,000	7.358	6.562	6.87	7.067	6.937	7.236	7.180
60,000	3.126	2.471	2.721	2.851	2.765	3.035	2.972
100,000	1.571	1.180	1.333	1.407	1.361	1.543	1.504
$\lambda_D = 20$							
1000	348.9	348.9	348.9	348.9	348.9	348.9	348.9
5000	94.25	94.23	94.09	94.20	94.22	94.25	94.25
10,000	46.49	46.29	46.20	46.41	46.37	46.46	46.46
30,000	12.50	11.73	12.00	12.22	12.10	12.38	12.34
60,000	4.861	4.151	4.411	4.566	4.469	4.757	4.692
100,000	2.302	1.859	2.024	2.115	2.061	2.261	2.218
$\lambda_D = 200$							
1000	4649	4649	4649	4649	4649	4649	4649
5000	628.3	628.3	628.2	628.3	628.3	628.3	628.3
10,000	230.2	230.1	229.9	230.1	230.1	230.2	230.2
30,000	40.87	40.16	40.36	40.61	40.48	40.76	40.73
60,000	12.85	12.12	12.36	12.55	12.44	12.74	12.67
100,000	5.341	4.862	5.025	5.137	5.076	5.288	5.246

The screening according to the three values of Debye length (λ_D) is given in each section of table

- the ion–ion interactions usually can be described by the exponentially screened Coulomb interaction but when the temperature is very high and/or the Debye length is small, then the real PECs should be used (at the small inter-atomic distances the PECs may significantly differ from the Coulomb one).

Supplementary material

Text files with PECs points for singly ionized system (NHp1.dat, NHp2.dat) and doubly ionized system (NHpp1.dat, NHpp2.dat) are given; for the term symbols see figures 1 and 2).

Text files with $\sigma^2\Omega^{(1,1)*}$ and $\sigma^2\Omega^{(2,2)*}$ collision integrals: NHp_GROUND_ALLTEMPS.dat, NHp_EXCITED_ALLTEMPS.dat, NHpp_ALLTEMPS.dat to which function in the Appendix were fitted.

The file NHppCoulombExe.py for the collision integrals based on the screened Coulomb and screened exact N^+-H^+ interactions (two lowest dissociation channels)—run in terminal as: python3 NHppCoulombExe.py (NHpp1.dat, NHpp2.dat files are needed for running the code); if Python3 is installed.

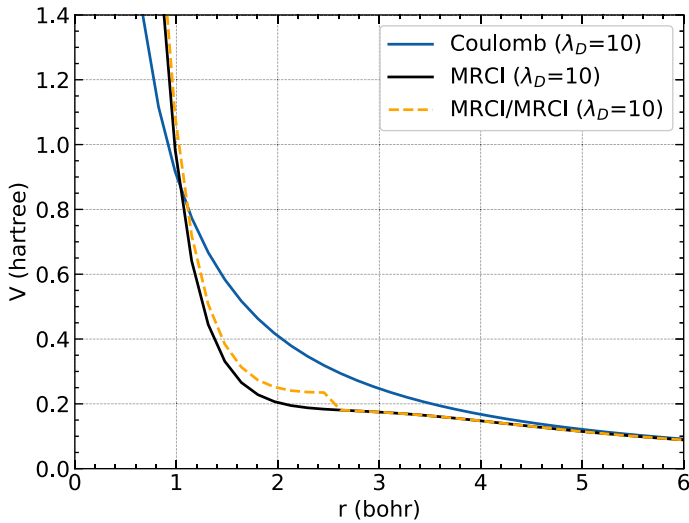


Fig. 8 Comparison of the Coulomb screened potential (Coulomb ($\lambda_D = 10$)), the MRCI screened potential (MRCI ($\lambda_D = 10$)), and theoretically preferred picewise MRCI/MRCI screened potential (MRCI/MRCI ($\lambda_D = 10$))

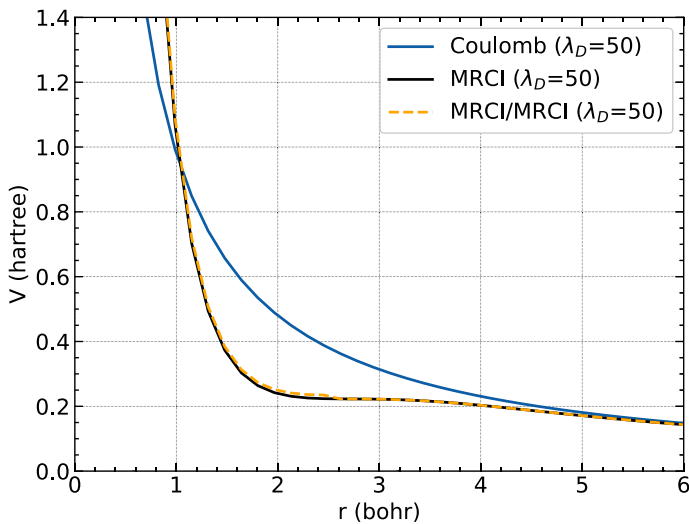


Fig. 9 Comparison of the Coulomb screened potential (Coulomb ($\lambda_D = 50$)), the MRCI screened potential (MRCI ($\lambda_D = 50$)), and theoretically preferred picewise MRCI/MRCI screened potential (MRCI/MRCI ($\lambda_D = 50$))

Appendix

The analytical fits for calculated collision integrals (weighted average are used in case of inter-atomic interaction by more than one PEC) are given below.

The collision integrals fits for the $N(^4S)-H^+$ interaction (1000–60,000 K):

$$f_{\sigma^2\Omega(1,1)^*}(T) = 11.43058 - 9.749665 \cdot 10^{-4}T + 3.542191 \cdot 10^{-8}T^2 - 5.832230 \cdot 10^{-13}T^3 + 3.560750 \cdot 10^{-18}T^4 + 1.981021 \cdot 10^4/T - 9.406998 \cdot 10^6/T^2,$$

$$f_{\sigma^2\Omega(2,2)^*}(T) = 13.24148 - 9.374457 \cdot 10^{-4}T + 2.993388 \cdot 10^{-8}T^2 - 4.482098 \cdot 10^{-13}T^3 + 2.548425 \cdot 10^{-18}T^4 + 4.788077 \cdot 10^3/T + 7.629800 \cdot 10^4/T^2,$$

The collision integrals fits for the H(2S)-N+(3P) interaction (1000–60,000 K):

$$f_{\sigma^2\Omega(1,1)^*}(T) = 6.738109 - 4.142295 \cdot 10^{-4}T + 1.324764 \cdot 10^{-8}T^2 - 2.04839 \cdot 10^{-13}T^3 + 1.206779 \cdot 10^{-18}T^4 + 6.209253 \cdot 10^3/T - 1.826268 \cdot 10^6/T^2,$$

$$f_{\sigma^2\Omega(2,2)^*}(T) = 7.478854 - 3.643781 \cdot 10^{-4}T + 9.712507 \cdot 10^{-9}T^2 - 1.309082 \cdot 10^{-13}T^3 + 6.952089 \cdot 10^{-19}T^4 + 3.341879 \cdot 10^3/T + 1.178651 \cdot 10^5/T^2,$$

The collision integrals fits for the N(2D)–H+ interaction (1000–60,000 K):

$$f_{\sigma^2\Omega(1,1)^*}(T) = 7.845238 - 6.309602 \cdot 10^{-4}T + 2.321091 \cdot 10^{-8}T^2 - 3.890748 \cdot 10^{-13}T^3 + 2.412083 \cdot 10^{-18}T^4 + 8.234410 \cdot 10^3/T - 2.754850 \cdot 10^6/T^2,$$

$$f_{\sigma^2\Omega(2,2)^*}(T) = 1.046621 - 7.583515 \cdot 10^{-4}T + 2.609569 \cdot 10^{-8}T^2 - 4.178571 \cdot 10^{-13}T^3 + 2.506631 \cdot 10^{-18}T^4 - 1.097175 \cdot 10^3/T + 3.775802 \cdot 10^6/T^2,$$

The collision integrals fits for the H(2S)-N+(1D) interaction (1000–60,000 K):

$$f_{\sigma^2\Omega(1,1)^*}(T) = 4.795429 - 2.712611 \cdot 10^{-4}T + 9.021328 \cdot 10^{-9}T^2 - 1.465565 \cdot 10^{-13}T^3 + 8.986424 \cdot 10^{-19}T^4 + 9.891191 \cdot 10^3/T - 4.252237 \cdot 10^6/T^2,$$

$$f_{\sigma^2\Omega(2,2)^*}(T) = 6.641164 - 3.680537 \cdot 10^{-4}T + 1.215349 \cdot 10^{-8}T^2 - 1.965340 \cdot 10^{-13}T^3 + 1.200023 \cdot 10^{-18}T^4 + 8.454778 \cdot 10^3/T + 3.545429 \cdot 10^6/T^2,$$

The collision integrals fits for the H(2S)-N2+(2P) interaction (1000–60,000 K):

$$f_{\sigma^2\Omega(1,1)^*}(T) = 16.59655 - 9.842176 \cdot 10^{-4}T + 3.029771 \cdot 10^{-8}T^2 - 4.586200 \cdot 10^{-13}T^3 + 2.671284 \cdot 10^{-18}T^4 + 1.880143 \cdot 10^4/T - 7.440769 \cdot 10^6/T^2,$$

$$f_{\sigma^2\Omega(2,2)^*}(T) = 24.03245 - 1.368839 \cdot 10^{-3}T + 4.060837 \cdot 10^{-8}T^2 - 6.003811 \cdot 10^{-13}T^3 + 3.454673 \cdot 10^{-18}T^4 + 1.113732 \cdot 10^4/T - 3.630537 \cdot 10^6/T^2,$$

Supplementary Information The online version contains supplementary material available at <https://doi.org/10.1007/s11090-022-10302-x>.

Acknowledgements There is no financial support to declare.

Open Access This article is licensed under a Creative Commons Attribution 4.0 International License, which permits use, sharing, adaptation, distribution and reproduction in any medium or format, as long as you give appropriate credit to the original author(s) and the source, provide a link to the Creative Commons licence, and indicate if changes were made. The images or other third party material in this article are included in the article’s Creative Commons licence, unless indicated otherwise in a credit line to the material. If material is not included in the article’s Creative Commons licence and your intended use is not permitted by statutory regulation or exceeds the permitted use, you will need to obtain permission directly from the copyright holder. To view a copy of this licence, visit <http://creativecommons.org/licenses/by/4.0/>.

References

1. McQuarrie D (2017) *Statistical physics*. Viva Books, New Delhi
2. Michaud G, Alecian G, Richer J (2015) *Atomic diffusion in stars*. Springer, New York
3. Buchowiecki M, Szabo P (2022) Transport coefficients of plasmas in mixtures of nitrogen and hydrogen. *Plasma Sources Sci Technol* 31:045010
4. Jones E, Oliphant T, Peterson P et al (2001) *SciPy: open source scientific tools for Python* (2001)
5. Sourd B, Aubreton J, Elchinger MF, Labrot M, Michon U (2006) High temperature transport coefficients in e/c/h/n/o mixtures. *J Phys D Appl Phys* 39(6):1105
6. Colombo V, Ghedini E, Sanibondi E (2009) Two-temperature thermodynamic and transport properties of argon–hydrogen and nitrogen–hydrogen plasmas. *J Phys D Appl Phys* 42(5):055213
7. Murphy AB (2012) Transport coefficients of plasmas in mixtures of nitrogen and hydrogen. *Chem Phys* 398:64
8. Stallcop JR, Bauschlicher CW, Partridge H, Langhoff SR, Levin E (1992) Theoretical study of hydrogen and nitrogen interactions: N-h transport cross sections and collision integrals. *J Chem Phys* 97(8):5578
9. Levin E, Partridge H, Stallcop JR (1990) Collision integrals and high temperature transport properties for n–n, o–o, and n–o. *J Thermophys Heat Transf* 4(4):469
10. Stallcop JR, Partridge H, Levin E (1992) Collision integrals for the interaction of the ions of nitrogen and oxygen in a plasma at high temperatures and pressures. *Phys Fluids B* 4(2):386
11. Kim J, Kwon O, Park C (2006) A high temperature elastic collision model for DSMC based on collision integrals. <https://doi.org/10.2514/6.2006-3803>
12. Liu HPD, Verhaegen G (1970) Electronic states of ch and nh. *J Chem Phys* 53(2):735
13. Capitelli M, Celiberto R, Gorse C, Bruno D (1995) Transport properties of high temperature air components: a review. *Plasma Chem Plasma Process* 16(1):S267
14. Laricchiuta A, Bruno D, Capitelli M, Celiberto R, Gorse C, Pintus G (2008) Collision integrals of oxygen atoms and ions in electronically excited states. *Chem Phys* 344(1):13
15. Laricchiuta A, Pirani F, Colonna G, Bruno D, Gorse C, Celiberto R, Capitelli M (2009) Collision integrals for interactions involving atoms in electronically excited states. *J Phys Chem A* 113(52):15250
16. Ghorui S, Das AK (2013) Collision integrals for charged-charged interaction in two-temperature non-equilibrium plasma. *Phys Plasmas* 20(9):093504
17. Xia G, Han Y, Wu Q, Chen L, Zhou N (2017) Transport coefficients of two-temperature lithium plasma for space propulsion applications. *Plasma Chem Plasma Process* 37(6):1505–1522
18. Amero JM, Vázquez GJ (2005) Electronic structure of nh⁺: an ab initio study. *Int J Quant Chem* 101(4):396
19. Zhang QQ, Yang CL, Wang MS, Ma XG, Liu WW (2017) Spectroscopic parameters of the low-lying electronic states and laser cooling feasibility of nh⁺ cation and nh⁻ anion. *Spectrochim Acta A Mol Biomol Spectrosc* 185:365
20. Sabzyan H, Keshavarz E, Noorisafa Z (2014) Diatomic dications and dianions. *J Iran Chem Soc* 11:871
21. Hamdan M, Mazumdar S, Marathe VR, Badrinathan C, Brenton AG, Mathur D (1998) Excited states of xh₂⁺(x=c, n, o, s) ions: a combined experimental and theoretical study. *J Phys B At Mol Opt Phys* 21:2571
22. Park JK, Sun H (1993) Valence electronic states of nh₂⁺ and ph₂⁺ dications. *Int J Quant Chem* 48:355
23. Wang F, Zhu Z, Jing F (1998) Analytic potential energy function for doubly charged ions bh₂⁺, ch₂⁺ and nh₂⁺. *J Mol Struct THEOCHEM* 453:71
24. Tuttle WD, Thorington RL, Viehland LA, Wright TG (2015) Interaction potentials, spectroscopy and transport properties of c+(2pj) and c+(4pj) with helium. *Mol Phys* 113(23):3767
25. Aissaoui L, Knowles PJ, Bouledroua M (2020) The role of spin-orbit effects in the mobility of n⁺ ions moving in a helium gas at low temperature. *Eur Phys J D* 74:155
26. Werner HJ, Knowles PJ, Manby FR, Black JA, Doll K, Heßelmann A, Kats D, Kähn A, Korona T, Kreplin DA, Ma Q, Müller TFI, Mitrushchenkov A, Peterson KA, Polyak I, Rauhut G, Sibaev M (2020) The molpro quantum chemistry package. *J Chem Phys* 152:144107
27. Friedrich H (2016) *Scattering theory*. Springer, Berlin
28. Kim SU, Monroe CW (2014) High-accuracy calculations of sixteen collision integrals for Lennard-Jones (12–6) gases and their interpolation to parameterize neon, argon, and krypton. *J Comput Phys* 273:358
29. Buchowiecki M (2022) High temperature collision integrals for m-6-8 and Hulburt-Hirschfelder potentials. *Int J Thermophys* 43:1–12

30. Wang WZ, Rong MZ, Yan JD, Murphy AB, Spencer JW (2011) Thermophysical properties of nitrogen plasmas under thermal equilibrium and non-equilibrium conditions. *Phys Plasmas* 18(11):113502
31. Kihara T, Taylor MH, Hirschfelder JO (1960) Transport properties for gases assuming inverse power intermolecular potentials. *Phys Fluids* 3(5):715
32. Capitelli M, Bruno D, Laricchiuta A (2013) *Fundamental aspects of plasma chemical physics: transport*. Springer, New York
33. Liboff RL (1959) Transport coefficients determined using the shielded coulomb potential. *Phys Fluids* 2(1):40
34. Mason EA, Munn RJ, Smith FJ (1967) Transport coefficients of ionized gases. *Phys Fluids* 10(8):1827
35. de Melo GF, Franzreb K, Ornellas FR (2021) Exploring the electronic states of the hydroxyl dication OH_2^+ : thermodynamic (meta)stability, bound-free emission spectra, and charge transfer processes. *Phys Chem Chem Phys* 23:13672
36. Li HW, Kar S (2012) Polarizabilities of Li and Na in Debye plasmas. *Phys Plasmas* 19(7):073303
37. Qi YY, Ning LN (2014) Dynamic processes and polarizability of sodium atom in Debye plasmas. *Phys Plasmas* 21(3):033301
38. Angel M, Montgomery H (2011) H_2^+ embedded in a Debye plasma: electronic and vibrational properties. *Phys Lett A* 375(17):1812
39. Janev R, Zhang S, Wang J (2016) Review of quantum collision dynamics in Debye plasmas. *Matter Radiat Extremes* 1(5):237
40. Wu C, Wu Y, Yan J, Chang TN, Gao X (2022) Transition energies and oscillator strengths for the intrashell and intershell transitions of the c-like ions in a thermodynamic equilibrium plasma environment. *Phys Rev E* 105:015206

Publisher's Note Springer Nature remains neutral with regard to jurisdictional claims in published maps and institutional affiliations.